scientific reports

Check for updates

OPEN

Multilocus phylogeny and phylogeographical patterns suggest the need for a comprehensive revision of the systematics of Stelliferinae Sasaki, 1989 (Sciaenidae, Acanthuriformes)

Tárcia Fernanda da Silva[1], Iracilda Sampaio[2], Arturo Angulo[3], Omar Domínguez-Domínguez[4] & Simoni Santos[1,5]✉

We evaluate the phylogenetic and phylogeographic patterns within Stelliferinae, the third most diversified subfamily in Sciaenidae, using a multilocus approach based on mitochondrial and nuclear markers, comprising 13 loci. Our results support the monophyly of Stelliferinae and the non-monophyly of *Stellifer*, whose species were grouped into three distinct clades, two of which were closely related to a clade encompassing *Bairdiella*, *Elattarchus*, *Odontoscion*, and *Corvula*. The monophyly of *Odontoscion* was rejected, since *Odontoscion xanthops* was found to be closer to *Corvula macrops* than to *Odontoscion dentex*, suggesting that both genera should be synonymized. In addition, our genetic inferences indicate that *Stellifer menezesi* and *Stellifer gomezi* represent a single species. Furthermore, *O. dentex* was grouped into two clades, one occurring in the Caribbean and another one on the Brazilian coast, which diverged ~ 3.3 million years ago (Ma), evidencing cryptic speciation likely driven by the Amazon River plume outflow. Our results suggest that Stelliferinae originated in the eastern Pacific around 16.7 Ma (13.2–20.3 Ma; Early Miocene) and subsequently colonized the western Atlantic during the Miocene and Pliocene, via the Central American Seaway, through multiple independent dispersal events. We also propose that the gradual rise of the Isthmus of Panama, which promoted changes in the oceanographic conditions in both the Pacific and Atlantic Oceans, played a key role in the diversification of these taxa. In conclusion, we suggest that a thorough taxonomic review of Stelliferinae is required.

Keywords Stelliferinae, Multiloci phylogeny, Speciation, Taxonomy, Phylogeography

Sciaenidae (Acanthuriformes) is a large family of fishes, comprising 68 genera and 298 species[1], widespread in the Atlantic, Pacific, and Indian oceans, inhabiting either tropical, subtropical or temperate regions[2,3]. Nonetheless, the diversification processes and the interrelationships among several taxa in Sciaenidae remain largely unknown. Even though previous phylogenetic inferences invariably support Sciaenidae as monophyletic[4,7], their intergeneric and interspecific relationships are poorly resolved, such as observed in taxa of the subfamily Stelliferinae[8,9].

[1]Laboratory of Fish Microbiology, Institute of Coastal Studies, Federal University of Para (UFPA), Alameda Leandro Ribeiro s/n, Braganca 68600-000, Para, Brazil. [2]Laboratory of Evolution, Institute of Coastal Studies, Federal University of Para (UFPA), Alameda Leandro Ribeiro s/n, Braganca 68600-000, Para, Brazil. [3]Escuela de Biología, Museo de Zoología/Centro de Investigación en Biodiversidad y Ecología Tropical (CIBET) and Centro de Investigación en Ciencias del Mar y Limnología (CIMAR), Universidad de Costa Rica, San Pedro de Montes de Oca, San José 11501, 2060, Costa Rica. [4]Laboratory of Aquatic Biology, Faculty of Biology, Universidad Michoacana de San Nicolás de Hidalgo (UMSNH), Morella, Michoacán, Mexico. [5]Laboratório de Microbiologia do Pescado, Instituto de Estudos Costeiros, Universidade Federal do Pará, Campus de Bragança, Alameda Leandro Ribeiro s/n, Aldeia, Bragança, Pará CEP 68600-000, Brazil. ✉email: simoni@ufpa.br

Stelliferinae was recognized as a supragenus[10], being later elevated to the subfamily level by Sasaki[11]. A total of 51 species distributed in the coast and estuaries along the western Atlantic and eastern Pacific belong to Stelliferinae, thus representing the third richest subfamily in Sciaenidae. Formerly, this subfamily comprised six genera, as follows: *Stellifer* Oken, 1817, *Ophioscion* Gill, 1863, *Bairdiella* Gill, 1861, *Odontoscion* Gill, 1862, *Corvula* Jordan and Eigenmann, 1889, and *Elattarchus* Jordan and Evermann, 1896. However, molecular phylogenetic inferences revealed the non-monophyly and the close relationship between *Stellifer* and *Ophioscion*, suggesting that both genera should be synonymized[8,9]. Recently, Chao et al.[12] followed this suggestion and recognized *Ophioscion* as a junior synonym of *Stellifer*, resulting in five valid genera of Stelliferinae.

All morphological and molecular phylogenetic studies confirmed the monophyly of Stelliferinae[6,8–11]. Nonetheless, the genetic and morphological similarities among taxa hindered the definition of reliable intergeneric and interspecific relationships within the subfamily, probably as a result to their rapid adaptive radiation[8,9]. Furthermore, to date, morphological and molecular phylogenetic analyses have evaluated only a limited number of Stelliferinae taxa, with just one study including all genera within the subfamily[11], thereby restricting the scope for comprehensive comparative analyses. A summary of previous phylogenetic studies is provided in Fig. 1.

Phylogenies based on morphological traits support the monophyly of the analyzed genera and confirm a close relationship between *Stellifer* and *Ophioscion*[10,11]. However, these studies differ regarding the placement of *Bairdiella*, which is identified as the sister group of *Odontoscion* in Chao[10], while is closely related to the *Stellifer/Ophioscion* clade in Sasaki[11]. Furthermore, Sasaki[11] proposed that *Odontoscion* is closely related to *Elattarchus* and that these genera form a clade with *Corvula*.

In contrast, molecular phylogenies including Stelliferinae suggest the non-monophyly of both *Stellifer* and *Ophioscion*[4,6,8,9]. The placement of *Bairdiella* also remains contentious in molecular analyses. Santos et al.[4] placed *Bairdiella* as closely related to the *Stellifer/Ophioscion* clade, while Barbosa et al.[8] identified it as the sister group of *Odontoscion*. In contrast, Lo et al.[6] and Silva et al.[9] proposed that *Bairdiella* forms a clade with *Corvula/Odontoscion*. Additionally, Lo et al.[6] reported a closer relatedness between one specimen of *Corvula macrops* Steindachner, 1875 and *Odontoscion xanthops* Gilbert, 1898 than to co-specific samples, suggesting the need for a re-evaluation of the taxonomic status of these taxa.

Another relevant aspect about the taxonomy of Stelliferinae is the hypothesis of hidden diversity in *Odontoscion*. A study based on DNA barcode revealed at least two lineages of *Odontoscion dentex* Cuvier, 1830 along the Atlantic, with a genetic divergence as high as 12.9%[13]. Likewise, species delimitation methods, using DNA barcoding, identified three cryptic lineages within *O. dentex* (two in the Caribbean coast and another one in the Brazilian coast), whose genetic differences ranged from 3.95 to 9.33%[14]. These results suggest that the taxonomic status of these lineages should be further investigated, given that only *O. dentex* is recognized for the western Atlantic[1].

The Stelliferinae subfamily has an amphi-American distribution, with species inhabiting estuarine and coastal regions of the western Atlantic and eastern Pacific, except for *O. dentex*, which is associated with coral reefs. Several Stelliferinae taxa are widely distributed across regions characterized by putative barriers to gene flow, which have been identified as key drivers of genetic differentiation and diversification in marine fishes. These barriers include marine circulation patterns, variations in salinity and sea surface temperature, freshwater and sediments plumes discharged from large rivers, and the formation of the Isthmus of Panama[15–18]. In the western Atlantic, the Amazon plume, formed between 9.4 and 2.4 Ma, discharges approximately 6,300 km^3 of freshwater and 900×10^6 tons of sediment annually into the ocean, extending about 2300 km along the northeastern coast of South America[19,20]. This plume acts as a significant barrier, preventing gene flow between populations and driving speciation among fishes in the Caribbean and Brazilian provinces[15,21,22]. Moreover, for amphi-American groups, the formation of the Isthmus of Panama (17 – 3 Ma) is considered a major event that triggered the diversification of marine biota in the region. It altered marine circulation, salinity, and temperature patterns in the western Atlantic and eastern Pacific, leading to isolation and diversification of marine species. Given that Stelliferinae taxa inhabit areas influenced by several historical and extant physical and ecological processes acting as barriers, it is necessary to evaluate the biogeographical structure of this group and investigate the potential barriers to gene flow and associated processes driving its diversification.

Therefore, considering: (i) the non-monophyly of *Stellifer*, (ii) the discrepancies in the phylogenies regarding the positioning of *Bairdiella* and *Odontoscion*, (iii) the lack of molecular phylogenies including *Elattarchus*, (iv) the need to evaluate the monophyly of *Corvula* and *Odontoscion* and (v) the debate about the taxonomic status of lineages in *O. dentex*, we carried out an extensive multilocus analysis in Stelliferinae based on mitochondrial and nuclear regions, totaling 13 genetic markers. The present data were used to infer the evolutionary relationships among the valid genera in this subfamily, to test the monophyly of *Stellifer*, *Corvula* and *Odontoscion*, to evaluate the positioning of *Bairdiella*, *Elattarchus* and *Odontoscion*, and to test the hypothesis of cryptic speciation in *O. dentex*. In addition, we also estimated the time of divergence, the biogeographic history, and phylogeographic patterns in Stelliferinae to infer the processes that shaped their diversification patterns.

Results

Phylogenetic relationships and the time of the most recent common ancestor (TMRCA)

The phylogenetic reconstruction was based on a dataset of 9,041 base pairs (bp) from the 13 genetic markers, referring to the three mitochondrial DNA and 10 nuclear DNA loci (Supplementary Table S1). A total of 66 specimens were used, representing 24 species distributed among the five valid genera of Stelliferinae (47% taxon coverage). In all analyses, *Larimus acclivis* and *Nebris microps* were used as outgroups.

In general, the topologies of concatenation-based (Maximum Likelihood - ML, Bayesian inference - BI and species tree in the StarBEAST) and the summary-coalescent species tree (ASTRAL) phylogenies were congruent, except for some discrepancies in some clades, and all our results supported the monophyletic status

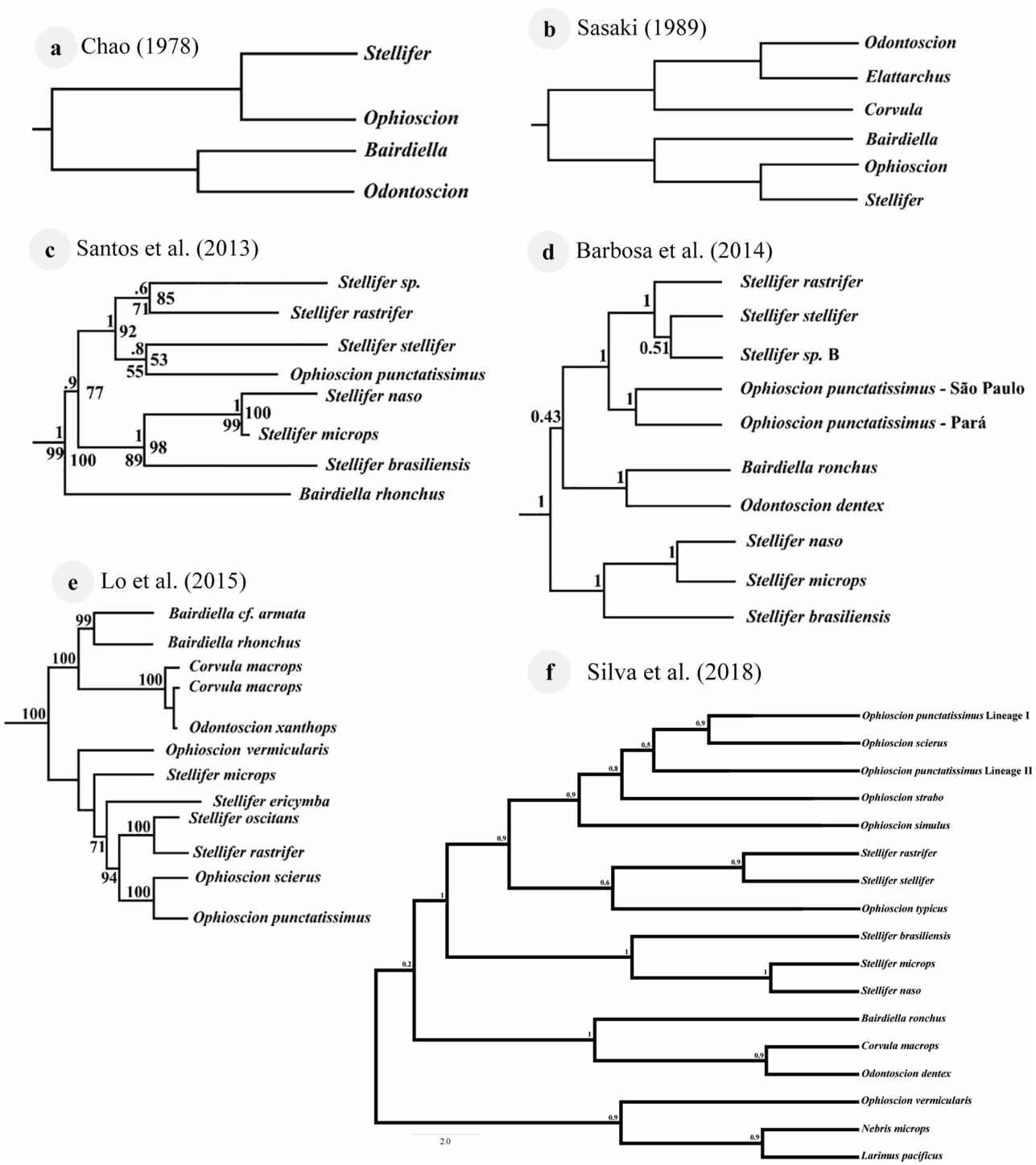

Fig. 1. Previous morphological (**a** and **b**) and molecular (c–f) phylogenetic hypotheses for Stelliferinae.

of Stelliferinae as well as the presence of four groups, each with high bootstrap, and posterior probabilities supports (Figs. 2, 3, 4 and 5). Group 1 indicates a close relatedness among *Bairdiella*, *Elattarchus*, *Corvula*, and *Odontoscion* while the groups 2 to 4 encompass species of *Stellifer*, suggesting that this is a non-monophyletic genus (Figs. 2, 3, 4 and 5). In ML and BI trees, groups 2 and 3 were closely related and formed a clade with group 1 (Figs. 2 and 3). On the other hand, in the concatenation-based species tree, group 2 was closely related to group 1 (Fig. 4), whereas the summary-coalescent species tree displayed a polytomic arrangement among groups 1, 2, and 3 (Fig. 5).

There was topological discordance among gene trees and phylogenies using the concatenation-based and the summary-coalescent approaches (Figs. 2, 3, 4 and 5; Supplementary Figs. 1–13). The mitochondrial markers support the four groups observed in the phylogenies based on concatenation or summary-coalescent approaches

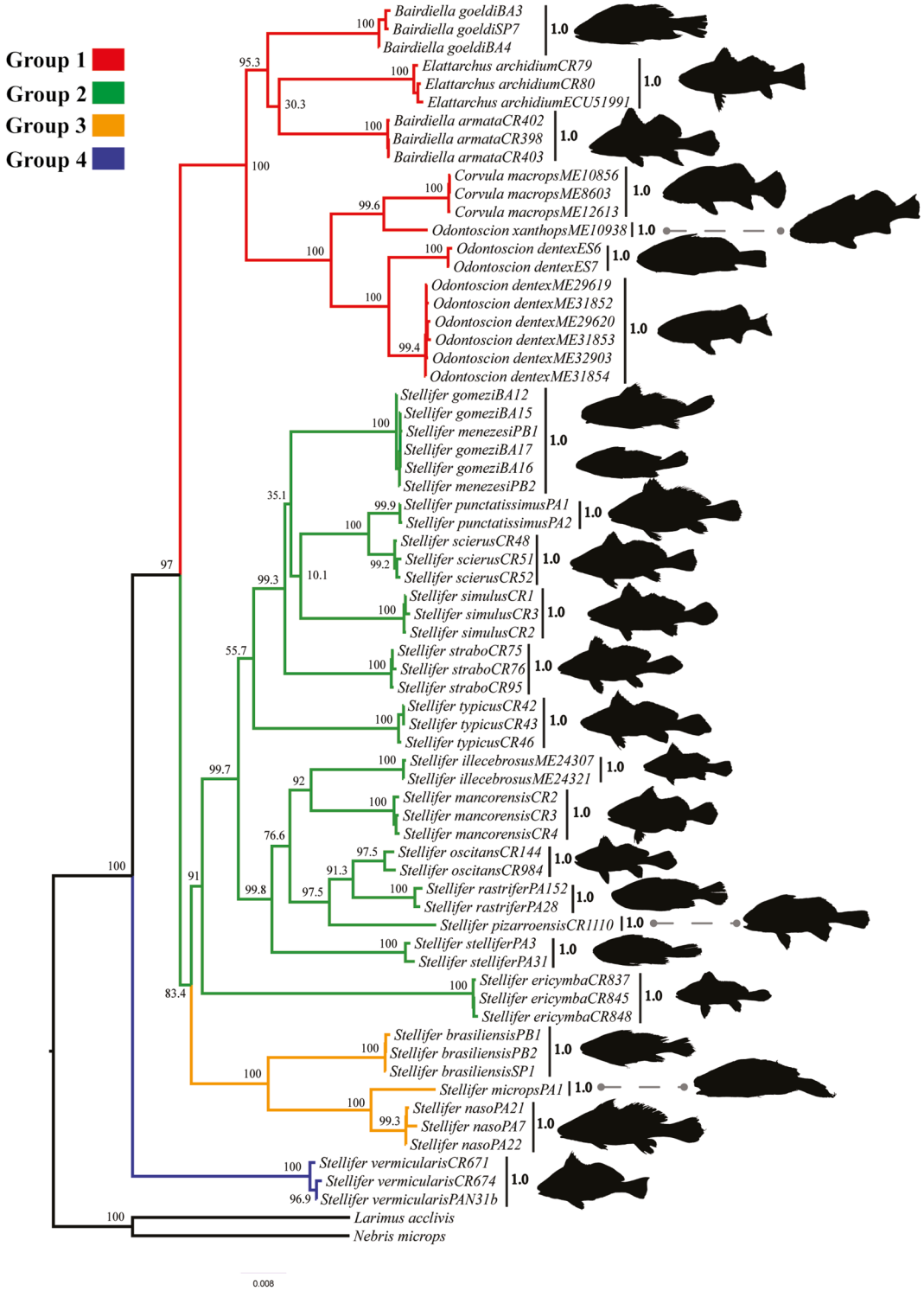

Fig. 2. Phylogenetic tree of Stelliferinae inferred from Maximum Likelihood (ML) based on the concatenated database of 13 genomic regions. The species *Larimus acclivis* and *Nebris microps* were used as outgroups. In the nodes are the bootstrap support values. The number after the vertical bars along each clade indicate the posterior probability values based on the Bayesian species delimitation.

(Supplementary Figs. 1–3). In contrast, the nuclear markers yielded poorly resolved trees, with all genera in a polytomic arrangement, and some gene trees grouping *Bairdiella*, *Elattarchus*, *Odontoscion* and *Corvula* in a clade with high bootstrap support (Supplementary Figs. 4–13).

In group 1, *Bairdiella* was recovered as the sister group of *Elattarchus*, while *Corvula* was closely related to *Odontoscion*. However, *Odontoscion* was found to be non-monophyletic, as *O. xanthops* was more closely

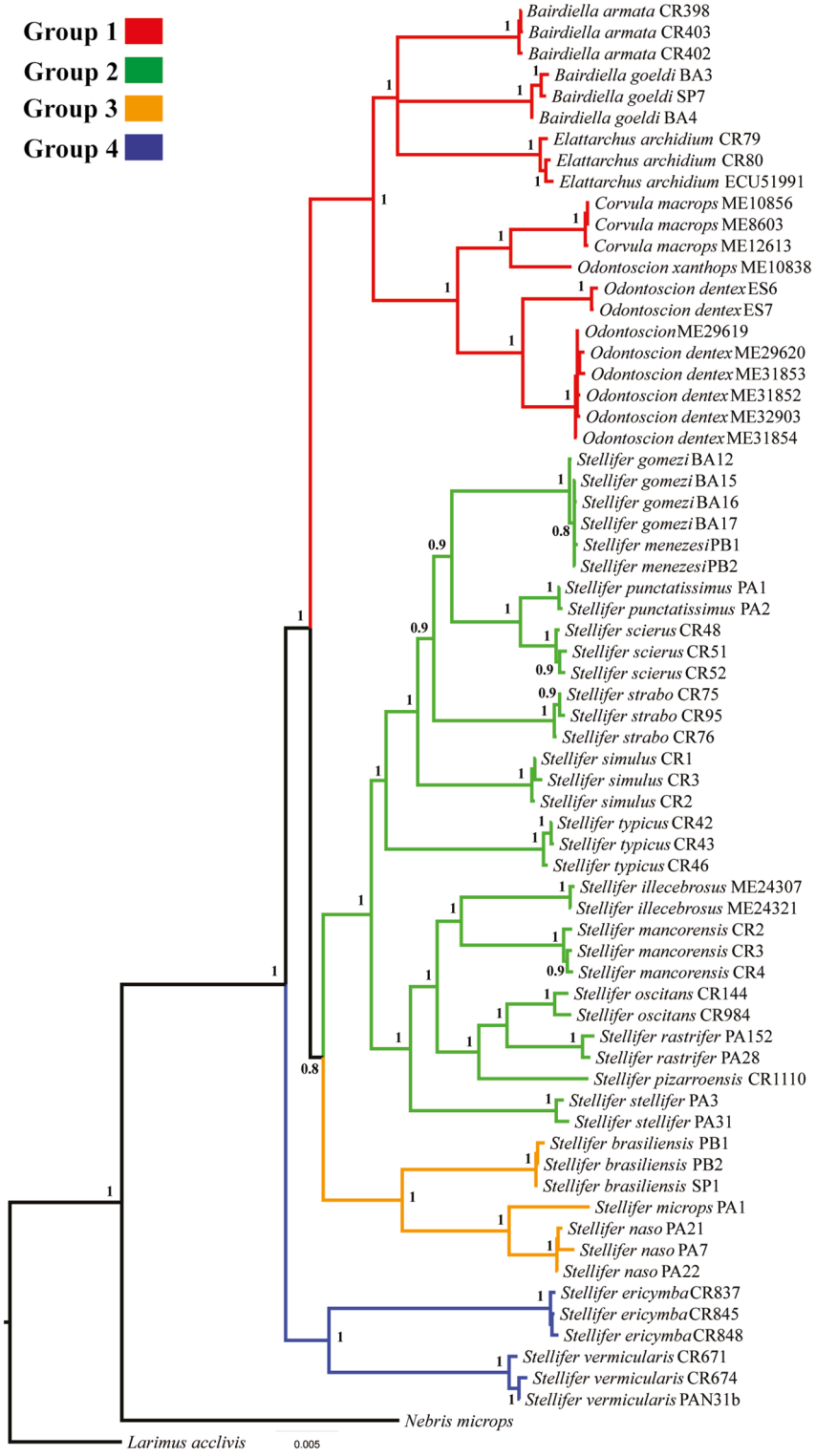

Fig. 3. Phylogenetic tree of Stelliferinae inferred using Bayesian Inference (BI) based on a concatenated database of 13 genomic regions. The species *Larimus acclivis* and *Nebris microps* were used as outgroups. The numbers on the nodes represent the posterior probability values.

related to *C. macrops* than to its congener *O. dentex*, except in the summary-coalescent species tree, where the *Odontoscion* species formed a clade but with low posterior probability (Figs. 2, 3, 4 and 5). In both concatenation-based and summary-coalescent species trees, *Bairdiella armata* Gill, 1863 was closely related to *Bairdiella goeldi* Marceniuk et al., 2019, although this relationship was well supported only in the concatenation-based species tree (Figs. 4 and 5). Conversely, *B. armata* was closely related to *Elattarchus archidium* Jordan and Gilbert,

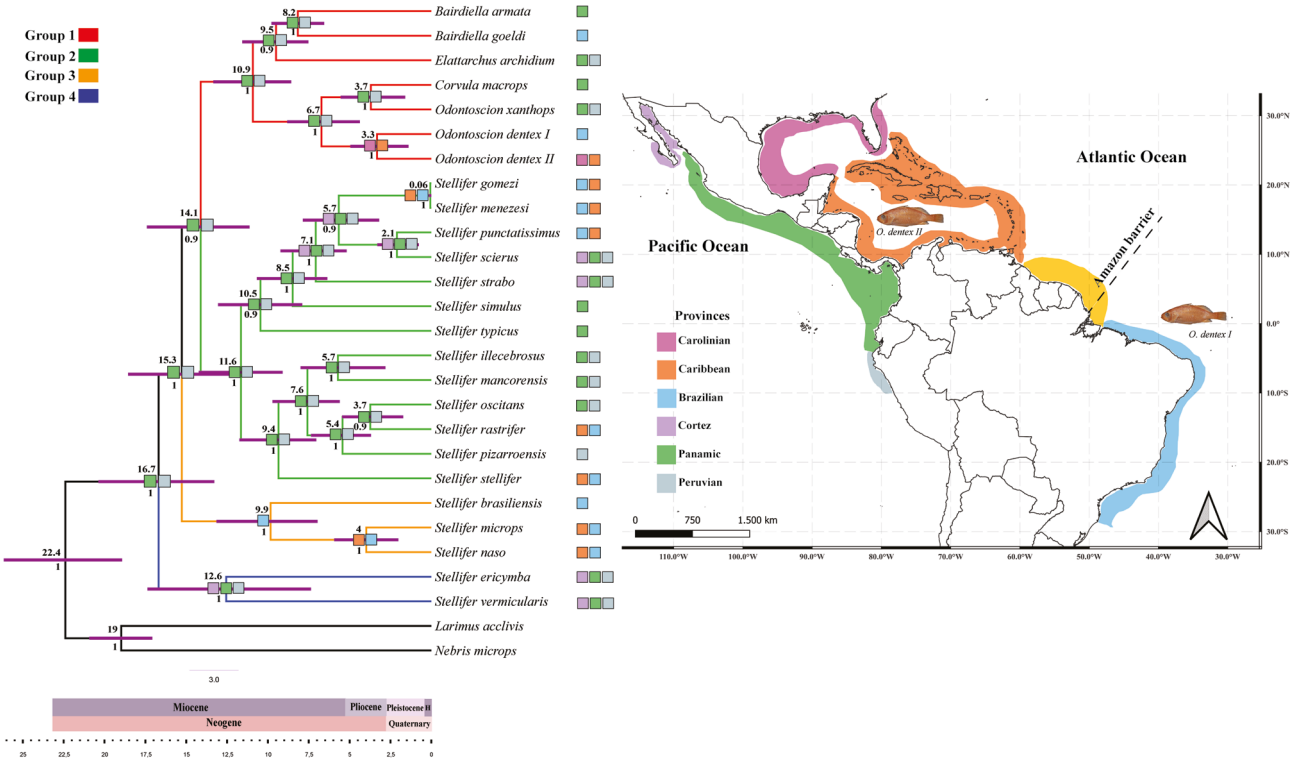

Fig. 4. Bayesian species tree with time-calibrated maximum clade credibility generated using StarBeast3 analysis, based on a concatenated dataset of 13 genomic regions from Stelliferinae. The species *Larimus acclivis* and *Nebris microps* were used as outgroups. Node squares represent ancestral range estimations, inferred using the BayArea-like + j identified as the best-fitting model by the biogeographic estimation. The time of the most recent common ancestor (TMRCA) is shown above the nodes, with bars representing the 95% highest posterior density intervals. Values below the nodes correspond to Bayesian posterior probabilities. The map shows the six marine biogeographic regions used to code the geographic distribution of extant species. **H** in the time bar refer to the Holocene.

1882 in the ML analysis, but with low bootstrap support (Fig. 2), and formed a polytomy with *B. goeldi* and *E. archidium* in the BI tree (Fig. 3). In addition, all phylogenetic inferences revealed two well-supported reciprocally monophyletic lineages within *O. dentex*, one occurring along the Mexican coast (Caribbean Province) and the other in the Brazilian Province (Figs. 2, 3, 4 and 5).

The non-monophyly of *Stellifer* was evident in all methods of phylogenetic reconstruction, as species from this genus grouped into three clades (Figs. 2, 3, 4 and 5). Within group 2, we identified two clades. In the first one *Stellifer punctatissimus* Meek and Hildebrand, 1925/*Stellifer scierus* Jordan and Gilbert, 1884 are sister taxa, and a close relationship was observed between *Stellifer gomezi* Cervigón, 2011/*Stellifer menezesi* Chao et al., 2021, both recovered as non-monophyletic taxa. Furthermore, this group also includes *Stellifer strabo* Gilbert, 1897, *Stellifer simulus* Gilbert, 1898, and *Stellifer typicus* Gill, 1863; however, the relationship among these taxa remains unresolved (Figs. 2, 3, 4 and 5). In the second clade of group 2, *Stellifer illecebrosus* Gilbert, 1898 and *Stellifer mancorensis* Chirichigno F., 1962 are sister taxa, forming a clade closely related to *Stellifer oscitans* Jordan and Gilbert, 1882/*Stellifer rastrifer* Jordan, 1889, and *Stellifer pizarroensis* Hildebrand, 1946, while *Stellifer stellifer* Bloch, 1790 is resolved as the earliest-diverging taxon in this group (Figs. 2, 3, 4 and 5).

In group 3, *Stellifer microps* Steindachner, 1864 was the sister taxon of *Stellifer naso* Jordan, 1889, forming a clade closely related to *Stellifer brasiliensis* Schultz, 1945 (Figs. 2, 3, 4 and 5). Finally, group 4 represents the most ancient clade within Stelliferinae in which *Stellifer ericymba* Jordan and Gilbert, 1882 and *Stellifer vermicularis* Günter, 1867 were closely related in both IB and concatenation-based species trees, with high support (Figs. 3 and 4). In contrast, in the ML and summary-coalescent species trees the group 4 contains only *S. vermicularis*, while *S. ericymba* is closely related to group 2 (Figs. 2 and 5).

The estimated TMRCA values indicate that the origin and diversification of Stelliferinae took place around 16.7 Ma (HPD: 13.2–20.3) during Early Miocene (Fig. 4), when most taxa diverged. Some taxa diverged later during the Pliocene while the diversification of *S. gomezi*/*S. menezesi* and *S. punctatissimus*/*S. scierus* occurred in the Pleistocene (Fig. 4).

Coalescent species delimitation

The tests carried out using distinct population size (θ) and root age (τ_0) parameters produced the same results, confirming that most nominal taxa in Stelliferinae correspond to valid species with a posterior probability of 1 (Fig. 2). In addition, the two phylogenetic lineages identified in *O. dentex* were recovered as distinct species by

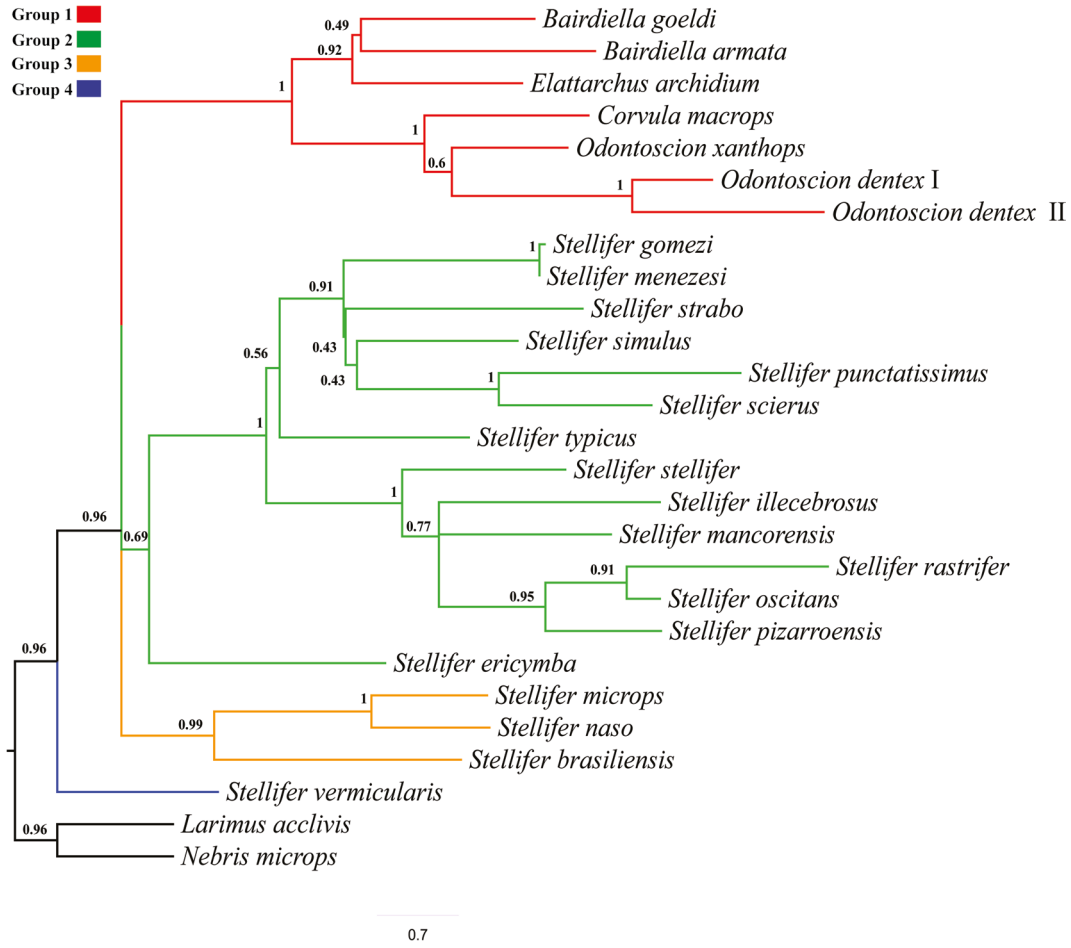

Fig. 5. Phylogenetic tree of Stelliferinae inferred using a summary-coalescent approach in ASTRAL-III based on a dataset of 13 genomic regions. The species *Larimus acclivis* and *Nebris microps* were used as outgroups. Node values represent bootstrap support greater than 30%.

BPP. Similarly, *C. macrops* and *O. xanthops* were also identified as unique species by this method. On the other hand, *S. gomezi* and *S. menezesi* were attributed to a single species.

Biogeographic history of Stelliferinae

The BioGeoBEARS analysis selected the BayArea-like + j as the best-fitting model for reconstructing the ancestral area of Stelliferinae, based on the corrected Akaike Information Criterion (Supplementary Table S2). According to this model, our analysis suggests that the Panamic and Peruvian provinces in the eastern Pacific were likely the center of origin for Stelliferinae during the Early Miocene. All groups appear to share an ancestor that inhabited the eastern Pacific before colonizing the western Atlantic. Our ancestral area reconstruction indicates at least five independent dispersal events from the eastern Pacific to the western Atlantic via the Central American Seaway (CAS) between the Miocene and Pliocene, prior to the closure of the Isthmus of Panama (Fig. 4). The ancestor of group 3 was the first to cross the CAS during Early Miocene, subsequently diversifying in the western Atlantic during Late Miocene. For group 1, the ancestral range was inferred to be in the Panamic and Peruvian provinces, followed by dispersal to the western Atlantic. This included ancestors that gave rise to the *B. goeldi* and *Odontoscion dentex* lineages, which occurred in distinct periods during the Late Miocene. The crown node of group 2 was estimated in the Panamic and Peruvian provinces, with two dispersal events to the western Atlantic. These events involved the ancestors of *S. menezesi*/*S. gomezi* and *S. punctatissimus* during the Late Miocene, and *S. rastrifer* during the Early Pliocene.

Discussion

Phylogenetic relationships and species delimitation in Stelliferinae

This study represents the most comprehensive molecular evaluation of the evolutionary relationships within Stelliferinae, considering both the taxa and molecular markers sampled. Our results support the monophyly of Stelliferinae, consistent with previous morphological and molecular phylogenetic studies[4,6,8–11].

The discordance between the topologies of gene trees and phylogenies inferred using concatenation and summary-coalescent approaches can be attributed to the limited phylogenetic signal present in individual markers. Moreover, topological incongruence may arise from incomplete lineage sorting, a phenomenon commonly

observed in taxa with large effective population sizes or recent rapid divergence events[23,24], as exemplified by Stelliferinae[8,9]. These processes frequently result in short, poorly resolved branches in phylogenetic trees[23,24]. While it remains challenging to determine which evolutionary processes have contributed most significantly to the observed phylogenetic patterns in Stelliferinae or to ascertain which method, coalescent or concatenation, is more prone to bias, evidence suggests that concatenation approaches have consistently provided robust insights into the phylogeny of taxa undergoing recent rapid radiations. These methods have been widely applied in systematic studies[23,24]. Accordingly, given that analyses of concatenated datasets yielded more congruent topologies, our discussion of taxonomic relationships within Stelliferinae is based on the results derived from these phylogenies.

In relation to group 1, all inferences corroborated a close relationship between *Bairdiella* and *Elattarchus*, while *Corvula* was placed as the sister group of *Odontoscion*. These results diverge from Chao[10] and Barbosa et al.[8] who suggested a close relationship between *Bairdiella* and *Odontoscion*. Nonetheless, representatives of *Corvula* and *Elattarchus* were not evaluated by these authors. Our results also differ from the proposal of Sasaki[11], who carried out the most comprehensive morphological phylogenetic analysis in Sciaenidae so far placing *Bairdiella* as the sister group of the clade *Stellifer*/*Ophioscion* (currently referred to as *Stellifer*). On the other hand, our results agree with Lo et al.[6] and Silva et al.[9] in relation to the close relationship between *Corvula* and *Odontoscion* and between this clade and *Bairdiella* (the genus *Elattarchus* was not included in their analyses). Therefore, considering that the present study is the only multilocus phylogenetic analysis in Stelliferinae including *Elattarchus*, we suggest that the relationships recovered in group 1 may be the most likely evolutionary scenario for this clade.

The monophyly of *Bairdiella* was well supported only in the concatenation-based species tree. In fact, this genus was regarded as monophyletic by Lo et al.[6], even though these authors have not analyzed representatives of the genus *Elattarchus*. Since *Bairdiella* encompasses seven valid species and only two of them were included in the present study, as well as in Lo et al.[6], further efforts in sampling and utilization of multilocus data are needed to properly assess the monophyletic status of the genus.

Our results indicate that *Odontoscion* is a non-monophyletic genus since *O. xanthops* was more closely related to *C. macrops* than to the congeneric *O. dentex*. Lo et al.[6] also found *O. xanthops* and *C. macrops* as closely related species based on their genetic similarity. Furthermore, a recent species delimitation study suggested that these taxa may represent a single species[14]. In fact, these genera are morphologically similar. According to Sasaki[11], the genus *Odontoscion* is characterized by two autapomorphies, the basisphenoid separated ventrally from parasphenoid and the levator operculi originating from the posttemporal, while *Corvula* lacks autapomorphic traits. Nevertheless, the main diagnostic trait used to distinguish these groups is the presence of canines in *Odontoscion*, which has determined cases of misidentification within *Odontoscion* and *Corvula* [see 3, 25]. Although our phylogenetic and species delimitation (BPP) analyses support *O. xanthops* and *C. macrops* as distinct species, the morphological characters used to delimit the genera appear to be inconsistent and unreliable.

A detailed morphological comparison reinforces this view, revealing extensive overlap between species of *Odontoscion* and *Corvula* in nearly all traits traditionally used in generic diagnoses within Sciaenidae (Supplementary Table S3). Both genera share key features such as the absence of mental barbels, a two-chambered swim bladder without appendages, and a finely serrated preopercular margin lacking strong bony spines[26,27]. They also exhibit similar body forms, with elongate profiles and terminal to subterminal mouths, as well as longitudinal stripes below the lateral line[25–27]. Dorsal fins are continuous in both groups, with overlapping counts of spines (10–13) and soft rays (21–29), and anal fins consistently bear two spines and 7 to 11 soft rays[26,27]. While differences such as the presence of canines in *Odontoscion* exist, they likely reflect intraspecific variability or ecological adaptations rather than deep phylogenetic divergence. Given the strong morphological congruence and the close evolutionary relationships inferred from molecular data, we propose that *Corvula* should be considered a junior synonym of *Odontoscion*.

Moreover, two reciprocally monophyletic lineages were identified in *O. dentex* following a disjunct distribution range since each lineage was restricted to distinct provinces (Brazilian and the Caribbean). Likewise, a report based on DNA barcoding[13] recovered two genetically divergent groups (12.9%) between samples from the Caribbean and Brazil in this taxon. Later, species delimitation analysis using DNA barcoding identified three putative species in *O. dentex*; one of them endemic to the Brazilian province while the remaining two were distributed along the Caribbean province[14]. So far, three valid species are recognized in *Odontoscion*, including two taxa from the eastern Pacific (*O. xanthops* and *Odontoscion eurymesops* Heller and Snodgrass, 1903) and a single taxon described for the western Atlantic (*O. dentex*). Thus, the present results and DNA barcoding strongly indicates a cryptic speciation process within *O. dentex*. Accordingly, a detailed taxonomic review based on morphological data and increased sampling efforts is necessary to validate the new species of *Odontoscion* along the western Atlantic.

The non-monophyly in the genus *Stellifer* was evident by all analyses based on molecular data[4,6,8,9], thereby diverging from morphological phylogenetic inferences[10,11]. Based on a multilocus approach, Silva et al.[9] proposed that *Stellifer* and *Ophioscion* were closely related groups that should be synonymized, while Chao et al.[12] placed *Ophioscion* as a junior synonym of *Stellifer*. However, our phylogenetic analysis revealed three groups within *Stellifer*, where the groups 2 and 3 would be more related to the species in group 1 (along with *Bairdiella*, *Elattarchus*, *Corvula*, and *Odontoscion*) than to group 4. In addition, the group 4 represented the most divergent clade within Stelliferinae, as also reported by Lo et al.[6] and Silva et al.[9]. Based on the congruent results between this study and previous reports[4,6,8,9], we recommend that these groups should be reclassified as distinct genera of Stelliferinae. For that, all recognized species in *Stellifer* should be sampled to carry out a wide taxonomic revision in this subfamily, focused on the classification of new or previous valid genera.

In addition, *S. gomezi* and *S. menezesi* are non-monophyletic species, as they formed a highly supported polytomous branch in the present study. *Stellifer menezesi* is a recently described species[12], differentiated from

S. gomezi by variations in body height, size of nostrils, length of snout, pectoral fins, and second spine of the anal fin; even though, most of morphological traits are overlapped in both taxa[12,28]. Furthermore, the Bayesian Phylogenetics and Phylogeography (BPP) test also recovered *S. gomezi* and *S. menezesi* as a single species, consistent with previous findings from other species delimitation methods[14]. Therefore, we provide additional evidence that *S. menezesi* should be considered a junior synonym of *S. gomezi*.

In group 2, *S. menezesi/S. gomezi*, *S. scierus/S. punctatissimus*, *S. strabo*, and *S. simulus* were recovered as closely related species, forming a well-supported clade, corroborating the phylogenetic inferences by Silva et al.[9]. On the other hand, *S. typicus* was closely related to this clade, while Silva et al.[9] proposed that *S. rastrifer/S. stellifer* is a sister clade of the group comprising *S. menezesi/S. gomezi*, *S. scierus/S. punctatissimus*, *S. strabo*, and *S. simulus*. Nevertheless, the support values of these evolutionary relationships were low in both reports, thus hindering the determination of the most likely phylogenetic arrangement among such species.

Furthermore, the group 2 revealed a close and highly supported relationship among *S. oscitans*, *S. rastrifer*, and *S. pizarroensis*. These taxa formed a clade along with *S. illecebrosus* and *S. mancorensis*, while *S. stellifer* was the most divergent species in this group. These results differ from previous phylogenetic studies based on a few species of the genus, which have shown incongruent results. For instance, Santos et al.[4] recovered *S. rastrifer* as the sister group of *Stellifer* sp. B (currently referred to as *Stellifer collettei*), while *S. stellifer* was the sister group of *S. punctatissimus* (formerly *Ophioscion punctatissimus*). On the other hand, Barbosa et al.[8] suggested a close relationship between *S. stellifer* and *Stellifer* sp. B, both forming a clade with *S. rastrifer*. Instead, Lo et al.[6] suggested that *S. rastrifer* is closely related to *S. oscitans*, while Silva et al.[9] allocated *S. rastrifer* as the sister group of *S. stellifer*. Considering the reduced number of species in previous studies and the strong statistical support obtained in our analyses, we suggest that the present phylogenetic arrangement should be the most likely scenario for these taxa.

In the case of group 3, we observed that *S. microps* and *S. naso* formed a closely related clade, grouped along with *S. brasiliensis*, as previously reported in other molecular phylogenies including these species[4,8,9]. Therefore, our results reinforce that such clade of *Stellifer* should be referred to as a distinct genus.

Time of diversification, biogeographic history and phylogeographic patterns in stelliferinae

Our results suggested that Stelliferinae fishes originated in Early Miocene, about 16.7 Ma (HPD: 13.2–20.3 Ma). In addition, most taxa from this subfamily have also diverged during this period, with a few records of speciation during the Pliocene and Pleistocene. Similarly, Lo et al.[6] and Silva et al.[9] reported that the diversification of Stelliferinae has taken place during the Miocene, at 15.7 and 15.6 Ma, respectively.

The subfamily Stelliferinae exhibits an amphi-American distribution. From a phylogeographic perspective, we identified closely related species inhabiting distinct oceans within groups 1 and 2. Range estimations suggest that the center of origin for Stelliferinae was in the eastern Pacific. Our findings are consistent with those of Lo et al.[6], who also proposed an eastern Pacific origin for Stelliferinae. Based on our ancestral reconstruction, we propose that the ancestors of Stelliferinae species diversified in the Pacific and that multiple independent dispersal events to the western Atlantic occurred between the Miocene and Pliocene, via the CAS, prior to the closure of the Isthmus of Panama. Several studies have suggested that the CAS served as the primary dispersal route for marine biota between the Pacific and Atlantic prior to the closure of the Isthmus[16,18,29].

The formation of the Isthmus of Panama was a gradual process that began in the Miocene (~17 Ma) and culminated in the complete isolation of the Pacific and Atlantic Oceans approximately 3 Ma during the Pliocene[17,18,30]. Throughout the Miocene and Pliocene, tectonic movements drove the uplift of the Isthmus and the progressive closure of the CAS, the Pacific-Atlantic connection route in Central America. The reduced connectivity between these oceans led to significant changes in oceanographic conditions, including alterations in sea surface circulation patterns, salinity, and temperature[17,18,30–32], which would have favored the occurrence of diversification events within Stelliferinae. However, a partial connection between the eastern Pacific and western Atlantic persisted until the total closure of the Isthmus of Panama (~3 Ma), being putatively sufficient to enable species dispersal between the two regions. This scenario could explain the formation of closely related clades among species now distributed in geographically disjunct areas.

It is noteworthy that the divergence between *S. punctatissimus* and *S. scierus* dated back to nearly 2.1 Ma during the Pleistocene, with the 95% highest posterior density (HPD: 0.7–3.3 Ma) overlapping the diversification times reported in previous studies[6,9]. Accordingly, we suggest that the closure of the Isthmus of Panama might have interrupted the gene flow between ancestral populations, leading them to independent evolutionary pathways that promoted the speciation, as proposed by Silva et al.[9]. In fact, several authors suggest that the closure of the Isthmus of Panama was the most important vicariant event to the speciation processes among marine sister taxa of amphi-American distribution[16,33–36].

The divergence between the two lineages of *O. dentex* occurred approximately 3.3 Ma (HPD: 1.4–4.9), during the Pliocene, following a disjunct distribution, with one lineage occurring in the Brazilian province and another in the Caribbean province. It is noteworthy that *O. dentex* is a species associated with coral reefs, being found at depths of up to 30 m[37], inhabiting areas of high salinity. It is likely that this taxon has low tolerance to reduced salinity levels, a characteristic commonly observed in coastal and estuarine environments where most species of Sciaenidae occur. Moreover, the two lineages of *O. dentex* are separated by the Amazon plume, a massive outflow of freshwater and sediment from the Amazon River into the Atlantic that represents a major biogeographic barrier for Atlantic reef fishes[15,21,22]. Interestingly, the estimated divergence time between the two lineages coincides with the period of increased Amazon River outflow (6.8 to 2.4 Ma) during the Late Miocene and Early Pliocene[19]. This enhanced outflow likely acted as a barrier, isolating populations of *O. dentex* in the Caribbean and Brazilian provinces, thereby preventing gene flow and promoting speciation.

The period from 6.8 to 2.4 Ma is recognized as the second stage of Amazon River formation, marked by an increase in freshwater and sediment discharge into the western Atlantic, with sedimentation rates

reaching ~ 0.3 m/ka[19]. From 2.4 Ma onwards, sedimentation rates into the Atlantic increased significantly to ~ 1.2 m/ka, coinciding with the Amazon River attaining its current conformation[19]. Today, the Amazon River discharges approximately 6300 km^3 of freshwater and 900×10^6 tons of sediment annually into the western Atlantic[20]. The area of influence of the Amazon River plume extends roughly 200 km from its mouth, reducing salinity levels up to an isobath of 30 m deep in the Atlantic Ocean[38–40]. Consequently, the Amazon River plume has prevented the formation of reef habitats at these depths, acting as a potential barrier to the dispersal of *O. dentex* lineages. Supporting this hypothesis, several studies on coral reef fishes have demonstrated the role of the Amazon plume in driving diversification among sister species distributed between the Caribbean and Brazilian provinces[15,21,41–43]. Therefore, our results suggest the existence of at least two species within *O. dentex*, underscoring the need for additional sampling across its distribution range to refine biogeographic inferences and conduct a comprehensive taxonomic review of this nominal taxon.

Conclusions

Our study represents a substantial advancement in the systematics of Stelliferinae by combining broader taxonomic sampling, expanded genetic data, and integrated phylogenetic and biogeographic analyses. In summary, our results confirm the monophyly of Stelliferinae, while the genera *Odontoscion* and *Stellifer* proved to be non-monophyletic, and cryptic diversity was detected within *O. dentex*. Conversely, *S. gomezi* and *S. menezesi* are likely to represent a single species, and the genera *Corvula* and *Odontoscion* should be synonymized. Additionally, our ancestral area reconstruction suggests an eastern Pacific origin to Stelliferinae, where ancestral lineages diversified and undertook independent dispersal events to colonize the western Atlantic. Moreover, the formation of the Isthmus of Panama appears to have played a role in the diversification of Stelliferinae. The Amazon plume outflow was also identified as a likely barrier driving diversification in *O. dentex*. Therefore, this study provides evidence supporting the need for a comprehensive taxonomic review of Stelliferinae.

Materials and methods

Sample collection

We sampled 24 of the 51 valid species of Stelliferinae, representing 47% taxon coverage and including all currently genera recognized in this subfamily: *Stellifer* (18/31 species), *Bairdiella* (2/7 species), *Odontoscion* (2/3 species), *Corvula* (1/3 species), and *Elattarchus* (1/1 species). Samples were collected from sites across the western Atlantic and eastern Pacific (Table 1). Species selection was guided by morphological diversity, taxonomic breadth, and the availability of high-quality tissue samples. Although not comprehensive, this sampling provides a robust framework for phylogenetic analyses and supports the taxonomic reassessment of the subfamily.

In total, 66 specimens were analyzed. These included 24 samples obtained from the tissue bank of Sciaenidae available in the Laboratory of Fish Microbiology at the Institute of Coastal Studies, Federal University of Para (UFPA), Brazil; 29 samples from the fish collection at the Museum of Zoology, University of Costa Rica (UCR); and 13 samples from the fish collection at the Universidad Michoacana de San Nicolás de Hidalgo (UMSNH), Mexico. As outgroups, we included samples of *Larimus acclivis* Jordan and Bristol, 1898 and *Nebris microps* Cuvier, 1830 (Table 1). All specimens were identified based on identification keys[10,44–46].

No threatened or protected species were used in the present study. The specimens sampled along the Brazilian coast were collected by artisanal fisheries under license provided by the Brazilian Environment Ministry (Permit number 18401-3) on behalf of Dr. Simoni Santos. The samples from Costa Rica were collected according to the licenses obtained from the National System of Conservation Areas (Permit code R-SINAC-SE-DT-PI-003-2021) and the National Council of Biodiversity Management (Permit code R056-2015-OT-CONAGEBIO) as well as the resolution No. 377 of the Vicerectoría de Investigación of the UCR. The specimens from Mexico were collected under permits PPF/DGOPA-035/15 and CONAPESCA-PPF/DGOPA-262/17, while the fishes from Ecuador at the UMSNH were collected according to the license 013/2012 PNG/N21-2017-EXP-CM-2016-DNB/MA.

Ethics declaration

For the sampling, approval by the ethics committee was not requested because the fish were purchased from artisanal fishermen and were already dead at the time of collection.

DNA extraction, polymerase chain reaction amplification, and sequencing of genomic regions

The whole genomic DNA was isolated from muscle tissue using the Wizard Genomic DNA Purification kit (PROMEGA). The concentration and the purity of DNA samples were evaluated in a Nanodrop 2000 spectrophotometer (Thermo Scientific).

The 13 DNA markers were amplified via Polymerase Chain Reaction (PCR), comprising three mitochondrial (16S rDNA, COI, and CYTB) and ten nuclear (RHOD, EGR1, RAG1, ENCI, SREB2, GLYT, PLAG2, MYH6, ZICI, and TBRI) loci. Out of this total, 12 markers refer to exons while one of them (16S rDNA) represents a non-protein-coding gene. The PCR was carried out 2.4 µl of dNTPs at 1.25 mM, 1.5 µl of 10x buffer solution, 0.5 µl of $MgCl_2$ at 50 mM, 0.3 µl of each primer at 10 pmol/µl, 1–3 µl of template DNA (100 ng/µl), 0.12 µl of *Taq* DNA polymerase at 5U/µl (Invitrogen - Thermo Fisher Scientific) and ultrapure water to a final volume of 15 µl. A nested PCR was carried out to amplify the RAG1 marker, as described by Silva et al.[9]. Details about the primers and the amplification conditions for each marker are shown in Table 2.

The quality of amplicons was evaluated by electrophoresis in 1% agarose gel stained with GelRed and visualized under ultraviolet light. The successfully amplified PCR products were purified using the polyethylene glycol-8000 M protocol[55]. The sequences were generated by Sanger's method[56] using the Big Dye 3.1 terminator

kit (Applied Biosystems) according to the manufacturer's instructions. The sequencing was performed in ABI 3500XL Genetic Analyzer (Applied Biosystems).

Phylogenetic inferences and time of the most recent common ancestor (TMRCA)

The sequences were edited using the software Bioedit 5.0.6[57] and automatically aligned in Clustal W[58], available in Bioedit. Manual adjustments in the alignments were carried out when necessary. Degenerated bases were used in the heterozygous sites of nuclear regions. The database was concatenated in SequenceMatrix[59], while PartitionFinder 2[60] was used to select the best evolutionary models and partitions for Bayesian inference (BI).

Phylogenetic reconstruction based on Maximum Likelihood (ML) inference was performed with IQ-TREE 2.1.13[61] for the 13 individual markers and the concatenated dataset. Coding regions were partitioned by codon position, while a single partition was applied to the 16S rDNA, using evolutionary models selected by ModelFinder[62] (Supplementary Table S1). Branch support was evaluated through nonparametric bootstrapping, with 1000 replicates for individual markers and 2000 replicates for the concatenated dataset.

The BI tree was generated in the software MrBayes GPU[63,64]. In this case, the 12 protein-coding regions were partitioned according to their codon positions using the models selected by PartitionFinder, whereas the 16S rDNA sequences were considered a single partition (Supplementary Table S1). Four independent runs (30 million generations each) were carried out using the default parameters from each model as starting values. Clade posterior probabilities were calculated by using Metropolis coupled Markov Chain Monte Carlo algorithm (MCMCMC), assuming a burn-in of 10%. The run parameters over generations and the data convergence were evaluated in the software Tracer 1.7.1[65], where only ESS (Effective Sample Size) > 200 were accepted.

The species tree and the TMRCA in Stelliferinae were determined using StarBEAST3[66], available in the software BEAST 2.7.5[67]. For that, we considered the hierarchical BI based on HKY + I + G substitution model. The tree was built assuming an uncorrelated relaxed molecular clock and Yule prior. The time of divergence was calibrated based on the fossil record of Stelliferinae and *Larimus* Cuvier, 1830, a Sciaenid genus closely related to this subfamily. The TMRCA of the clade encompassing *Larimus* and *Nebris* Cuvier, 1830 was estimated from the fossils *Larimus henrici* Nolf and Aguilera, 1998 and *Larimus steurbauti* Nolf and Aguilera, 1998 found in the Cantaure formation, Mexico, dating back to 16 and 23 Ma (Early Miocene)[68]. The fossil record of *Bairdiella* sp[69]. from the Tortonian (7.2 to 11.6 Ma) was selected to estimate the TMRCA of the clade comprising *Bairdiella*. The posterior probability parameters were evaluated using MCMC with 130 million generations in which the log parameters were sampled every 13,000 generations, assuming a burn-in of 10%. The run parameters and the convergence of the chains were verified in Tracer 1.7.1[65] and only ESS > 200 were considered. The consensus tree along with their support values and estimates of time of divergence was generated using the software TreeAnnotator 1.8.

To account for discordances between gene trees and the species tree, the gene trees estimated in IQ-TREE were analyzed using the multispecies coalescent species tree method in ASTRAL-III[70]. ASTRAL-III has been demonstrated to be an efficient summary method under various levels of incomplete lineage sorting[70], although it is sensitive to gene tree estimation error. Therefore, to minimize such errors, we analyzed the data after collapsing poorly supported relationships in the gene trees (bootstrap < 30%) using TreeGraph 2[71].

Finally, all trees were visualized in FigTree 1.4.4 (http://tree.bio.ed.ac.uk/software/figtree/) and saved as SVG files for edition in the software InkScape 1.1 (https://inkscape.org/pt-br/).

Coalescent species delimitation

The diversity and delimitation of the interspecific barriers within the Stelliferinae were assessed based on the multispecies coalescent model available in the software Bayesian Phylogenetics and Phylogeography (BPP)[72,73] using the reversible-jump Markov Chain Monte Carlo (rjMCMC) algorithm[72] and the topology of ML tree as input.

We also tested different combinations of ancestral population size (θs) and root age (τ0) priors in order to test their influence on species delimitation. Therefore, we evaluated scenarios characterized by either a small ancestral population (theta prior = 2, 2000) and deep divergences (tau prior = 1, 10) or a large ancestral population size (theta prior = 1, 10) and shallow divergences (tau prior = 2, 2000). In these cases, we carried out two runs combining the priors for ancestral population size and root age, based on 9×10^5 MCMC generations, sampled every two generations with a burn-in of 9×10^4 generations.

Biogeographic analyses

We used the R package BioGeoBEARS[74,75] to estimate the ancestral biogeographic ranges of Stelliferinae based on the time-calibrated phylogeny inferred in StarBEAST3. We reconstructed historical biogeography by considering the distribution of species included in our phylogeny across six biogeographic provinces: the Carolinian, Caribbean, and Brazilian provinces in the western Atlantic[31], and Cortez, Panamic, and Peruvian provinces in the eastern Pacific[76]. We employed the corrected Akaike Information criterion (AICc) to compare six biogeographic models: the dispersal, extinction and cladogenesis (DEC) model[77]; the dispersal-vicariance (DIVA-like) model[78]; the Bayesian estimation (BAYAREA-like) model[79]; and the three models above, incorporating the jump dispersal (j) parameter[80] (DEC + J; DIVA-like + J; BayArea-like + j).

Species	Ocean	*n*	GenBank accession number												
			16S rDNA	COI	CYTB	RHOD	EGR1	RAG1	ENCI	SREB2	GLYT	PLAG2	MYH6	ZICI	TBRI
Stellifer brasiliensis	WA	3	MG494838[a], PQ206209, PQ206210	KJ907243[a], OQ872178[a], OQ872179[a]	PQ186275-PQ186277	KJ907313[a], PQ186223, PQ186224	MG494962[a], PQ204851	KJ907347[a], PQ186194, PQ186195	PQ204902-PQ204904	PQ205263-PQ205265	PQ204964-PQ204966	PQ205081-PQ205083	PQ205021, PQ205022	PQ205197-PQ205199	PQ205142-PQ205144
Stellifer gomezi	WA	4	PQ206202-PQ206205	OQ872165[a]-OQ872167[a]	PQ186256-PQ186258	PQ186218-PQ186219	-	-	PQ204883-PQ204885	PQ205244-PQ205246	PQ204948	-	-	PQ205181	PQ205128
Stellifer menezesi	WA	2	MG494764[a], MG494765[a]	MG494844[a], MG494845[a], OQ872161[a] - OQ872164[a]	PQ186254, PQ186255	MG495005[a], MG495006[a]	MG494923[a], MG494924[a]	MG494975[a], MG494976[a]	PQ204881, PQ204882	PQ205242, PQ205243	PQ204946, PQ204947	PQ205063, PQ205064	PQ205006, PQ205007	PQ205179, PQ205180	PQ205126, PQ205127
Stellifer microps	WA	1	KJ907211[a]	KJ907246[a]	PQ186274	KJ907316[a]	MG494961[a]	KJ907348[a]	PQ204901	PQ205262	-	PQ205080	PQ205020	PQ205196	PQ205141
Stellifer naso	WA	3	MG494839[a], MG494840[a], PQ206211	MG494916[a], MG494917[a], OQ872180[a]	PQ186282 - PQ186284	MG495069[a], MG495070[a], PQ186225	MG494967[a], MG494968[a], PQ204852	PQ186197-PQ186199	PQ204909-PQ204911	PQ205270-PQ205272	PQ204971-PQ204973	PQ205088-PQ205090	PQ205027-PQ205029	PQ205204-PQ205206	PQ205149, PQ205150
Stellifer punctatissimus	WA	2	MG494760[a], KJ907205[a]	KJ907238[a], KJ907239[a]	PQ186252, PQ186253	KJ907308[a], KJ907309[a]	MG494918[a], MG494919[a]	KJ907343[a], KJ907344[a]	PQ204879, PQ204880	PQ205240, PQ205241	PQ204944, PQ204945	PQ205061, PQ205062	PQ205004, PQ205005	PQ205177, PQ205178	PQ205124, PQ205125
Stellifer rastrifer	WA	2	KJ907216[a], KJ907218[a]	KJ907251[a], KJ907253[a]	PQ186280, PQ186281	KJ907320[a], KJ907322[a]	MG494965[a], MG494966[a]	KJ907349[a], KJ907351[a]	PQ204907, PQ204908	PQ205268, PQ205269	PQ204969, PQ204970	PQ205086, PQ205087	PQ205025, PQ205026	PQ205202, PQ205203	PQ205147, PQ205148
Stellifer stellifer	WA	2	KJ907224[a], KJ907225[a]	KJ907262[a], KJ907263[a]	PQ186278, PQ186279	KJ907330[a], KJ907331[a]	MG494963[a], MG494964[a]	KJ907359[a], PQ186196	PQ204905, PQ204906	PQ205266, PQ205267	PQ204967-PQ204968	PQ205084, PQ205085	PQ205023, PQ205024	PQ205200, PQ205201	PQ205145, PQ205146
Stellifer ericymba	EP	3	PQ206215-PQ206217	OQ872186[a]-OQ872188[a]	PQ186290-PQ186292	PQ186230-PQ186231	PQ204856-PQ204858	PQ186203	PQ204917-PQ204919	PQ205278-PQ205280	PQ204977-PQ204979	PQ205096-PQ205098	PQ205033-PQ205035	PQ205212-PQ205214	PQ205153, PQ205154
Stellifer illecebrosus	EP	2	PQ206220, PQ206221	OQ872190[a], OQ872191[a]	PQ186293, PQ186294	PQ186232-PQ186233	PQ204859, PQ204860	PQ186204-PQ186205	PQ204920, PQ204921	PQ205281, PQ205282	PQ204981, PQ204982	PQ205099, PQ205100	PQ205037, PQ205038	PQ205215, PQ205216	PQ205155, PQ205156
Stellifer mancorensis	EP	3	PQ206212-PQ206214	PQ187889-PQ187890	PQ186287-PQ186289	PQ186227-PQ186229	PQ204853-PQ204855	PQ186200-PQ186202	PQ204914-PQ204916	PQ205275-PQ205277	PQ204974-PQ204976	PQ205093-PQ205095	PQ205030-PQ205032	PQ205209-PQ205211	-
Stellifer oscitans	EP	2	PQ206218, PQ206219	OQ872189[a]	PQ186285-PQ186286	PQ186226	-	-	PQ204912, PQ204913	PQ205273, PQ205274	PQ204980	PQ205091, PQ205092	PQ205036	PQ205207, PQ205208	PQ205151, PQ205152
Stellifer pizarroensis	EP	1	-	PQ187891	-	PQ186234	-	-	PQ204922	PQ205283	-	PQ205101	PQ205039	PQ205217	-
Stellifer scierus	EP	3	MG494822[a], MG494824[a], MG494825[a]	MG494899[a], MG494901[a], MG494902[a]	PQ186259 - PQ186261	MG495053[a], MG495055[a], MG495056[a]	MG494951[a], MG494953[a], MG494954[a]	MG494994[a]-MG494996[a]	PQ204886-PQ204888	PQ205247-PQ205249	PQ204949-PQ204951	PQ205065-PQ205067	PQ205008-PQ205010	PQ205182, PQ205183	PQ205129, PQ205130
Stellifer simulus	EP	3	MG494834[a]-MG494836[a]	MG494912[a]-MG494914[a]	PQ186268-PQ186270	MG495065[a]-MG495067[a]	PQ204846, PQ204847	PQ186189-PQ186191	PQ204895-PQ204897	PQ205256-PQ205258	PQ204958-PQ204960	PQ205074-PQ205076	PQ205014-PQ205016	PQ205190-PQ205192	PQ205137
Stellifer strabo	EP	3	MG494826[a]-MG494828[a]	MG494903[a]-MG494905[a]	PQ186262-PQ186264	MG495057[a]-MG495059[a]	MG494955[a], MG494956[a], PQ204845	MG494997[a]-MG494999[a]	PQ204889-PQ204891	PQ205250-PQ205252	PQ204952-PQ204954	PQ205068-PQ205070	-	PQ205184-PQ205186	PQ205131-PQ205133
Stellifer typicus	EP	3	MG494829[a], MG494830[a], MG494832[a]	MG494906[a], MG494907[a], MG494909[a]	PQ186265- PQ186267	MG495060[a]-MG495062[a]	MG494957[a], MG494958[a], MG494960[a]	MG495000[a], MG495001[a], PQ186188	PQ204892- PQ204894	PQ205253-PQ205255	PQ204955-PQ204957	PQ205071-PQ205073	PQ205011-PQ205013	PQ205187-PQ205189	PQ205134-PQ205136
Stellifer vermicularis	EP	3	PQ206206-PQ206208	OQ872173[a]-OQ872177[a]	PQ186271-PQ186273	PQ186220-PQ186222	PQ204848-PQ204850	PQ186192, PQ186193	PQ204898-PQ204900	PQ205259-PQ205261	PQ204961-PQ204963	PQ205077-PQ205079	PQ205017-PQ205019	PQ205193-PQ205195	PQ205138-PQ205140
Bairdiella goeldi	WA	3	KJ907198[a], PQ206222, PQ206223	KJ907231[a], OQ872192[a], OQ872194[a]	PQ186295-PQ186297	KJ907301[a], PQ186235, PQ186236	MG494969[a], PQ204861, PQ204862	KJ907337[a], PQ186206	PQ204923-PQ204925	PQ205284-PQ205286	PQ204983-PQ204985	PQ205102-PQ205104	PQ205040, PQ205041	PQ205218-PQ205220	PQ205157-PQ205159
Bairdiella armata	EP	3	PQ206224-PQ206226	OQ872195[a]-OQ872199[a]	PQ186298-PQ186300	PQ186237-PQ186239	PQ204863 -PQ204865	PQ186207-PQ186208	PQ204926-PQ204928	PQ205287-PQ205289	PQ204986-PQ204988	PQ205105-PQ205107	PQ205042-PQ205044	PQ205221-PQ205223	PQ205160-PQ205162

Continued

Species	Ocean	*n*	GenBank accession number												
			16S rDNA	COI	CYTB	RHOD	EGR1	RAG1	ENCI	SREB2	GLYT	PLAG2	MYH6	ZICI	TBRI
Odontoscion dentex	WA	8	KJ907200[a], KJ907201[a], PQ206227-PQ206232	KJ907233[a], KJ907234[a], OQ872200[a]-OQ872205[a]	PQ186301-PQ186308	KJ907303[a], KJ907304[a], PQ186240-PQ186244	MG494970[a], MG494971[a], PQ204866-PQ204871	KJ907338[a], KJ907339[a], PQ186209-PQ186212	PQ204929-PQ204935	PQ205290-PQ205297	PQ204989-PQ204996	PQ205108-PQ205115	PQ205045-PQ205052	PQ205224-PQ205231	PQ205163-PQ205169
Odontoscion xanthops	EP	1	PQ206233	OQ872206	PQ186309	PQ186245	PQ204872	-	PQ204936	PQ205298	PQ204997	PQ205116	PQ205053	PQ205232	PQ205170
Corvula macrops	EP	3	PQ206234-PQ206236	OQ872207[a]-OQ872214[a]	PQ186310-PQ186312	PQ186246-PQ186248	PQ204873-PQ204875	PQ186213	PQ204937-PQ204939	PQ205299-PQ205301	PQ204998-PQ205000	PQ205117-PQ205119	PQ205054-PQ205056	PQ205233-PQ205235	PQ205171-PQ205173
Elattarchus archidium	EP	3	PQ206237-PQ206239	OQ872215[a]-OQ872217[a]	PQ186313-PQ186315	PQ186249, PQ186250	PQ204876, PQ204877	PQ186214-PQ186216	PQ204940-PQ204942	PQ205302-PQ205304	PQ205001-PQ205003	PQ205120-PQ205122	PQ205057-PQ205059	PQ205236-PQ205238	PQ205174-PQ205176
Larimus acclivis	EP	1	PQ206240	PQ187892	PQ186316	PQ186251	PQ204878	PQ186217	PQ204943	PQ205305	-	PQ205123	PQ205060	PQ205239	-
Nebris microps	WA	1	JX903980[a]	KP722742[a]	KP722653[a]	KP723018[a]	MT879864[a]	KP722929[a]	-	-	-	-	-	-	-

Table 1. Samples and genetic markers used in the phylogenetic analyses of stelliferinae. The accession number of sequences deposited in GenBank are shown below each marker. The abbreviations WA and EP refer to Western Atlantic and Eastern pacific, respectively; n = number of individuals used in the analyses; 16S rDNA = 16S ribosomal RNA gene; coi = cytochrome oxidase C subunit I; cytb = cytochrome b; rhod = rhodopsin; EGR1 = early growth response 1 gene; RAG1 = recombination activating protein 1 gene; ENCI = ectodermal-neural cortex 1 gene; SREB2 = super conserved receptor expressed in brain 2; glyt = glycosyltransferase; PLAG2 = pleiomorphic adenoma gene-like 2; MYH6 = myosin, heavy polypeptide 6; zicI = zic family member I; TBRI = T-box brain I. [a]sequences obtained from GenBank while (-) indicates missing data.

Marker	Primer (5'–3')	Reference	Amplification protocol
COI	FishF1: TCAACCAACCACAAAGACATTGGCAC FishR1: TAGACTTCTGGGTGGCCAAAGAATCA	Ward et al.[47]	Initial denaturation at 94 °C for 3 min, 30 cycles at 94 °C for 40 s (denaturation), 59 °C for 30 s (hybridization) and 72 °C for 30 s (extension), plus a final extension at 72 °C for 7 min
CYTB	Fishcytb-F: ACCACCGTTGTTATTCAACTACAAGAAC Truccytb-R: CCGACTTCCGGATTACAAGACCG	Sevilla et al.[48]	Initial denaturation at 94 °C for 4 min, 30 cycles at 94 °C for 30 s (denaturation), 60 °C for 1 min (hybridization) and 72 °C for 1 min (extension), plus a final extension at 72 °C for 7 min
16S rDNA	L1987: GCCTCGCCTGTTTACCAAAAAC H2609: CCGGTCTGAACTCAGATCACGT	Adapted from Palumbi[49]	Initial denaturation at 94 °C for 3 min, 30 cycles at 94 °C for 20 s (denaturation), 50 °C for 30 s (hybridization) and 72 °C for 30 s (extension), plus a final extension at 72 °C for 7 min
RHOD	Rod-F2w: AGCAACTTCCGCTTCGGTGAGAA Rod-4R: CTGCTTGTTCATGCAGATGTAGAT	Sevilla et al.[48]	Initial denaturation at 95 °C for 7 min, 40 cycles at 94 °C for 30 s (denaturation), 59 °C for 30 s (hybridization) and 72 °C for 30 s (extension), plus a final extension at 72 °C for 7 min
EGR1	E1 290 F: TMTCTTACACAGGCCGYTTCAC E1 1118R: CTTCTTGTCCTTCTGCCGYAGRT	Chen et al.[50] Chen et al.[51]	Initial denaturation at 95 °C for 4 min, 40 cycles at 95 °C for 40 s (denaturation), 59 °C for 40 s (hybridization) and 72 °C for 90 s (extension), plus a final extension at 72 °C for 7 min
RAG1	2510 L: TGGCCATCCGGGTMAACAC 4090R: CTGAGTCCTTGTGAGCTTCCATRAAYTT	Li and Ortí[52] López et al.[53]	Initial denaturation at 94 °C for 5 min, 40 cycles at 94 °C for 30 s (denaturation), 58–60.6 °C for 40 s (hybridization) and 72 °C for 40 s (extension), plus a final extension at 72 °C for 10 min
	2533 L: CTGAGCTGCAGTCAGTACCATAAGATGT 4078R: TGAGCCTCCATGAACTTCTGAAGRTAYTT	López et al.[53]	
	2533 L: CTGAGCTGCAGTCAGTACCATAAGATGT 4090R: CTGAGTCCTTGTGAGCTTCCATRAAYTT	López et al.[53]	Initial denaturation at 94 °C for 5 min, 40 cycles at 94 °C for 30 s (denaturation), 58–60.6 °C for 40 s (hybridization) and 72 °C for 40 s (extension), plus a final extension at 72 °C for 10 min
ENCI	EncI-F85: GACATGCTGGAGTTTCAGGA EncI-R982: ACTTGTTRGCMACTGGGTCAAA	Li et al.[54]	Initial denaturation at 95 °C for 4 min, 40 cycles at 95 °C for 30 s (denaturation), 62 °C for 1 min (hybridization) and 72 °C for 90 s (extension), plus a final extension at 72 °C for 5 min
SREB2	Sreb2-F10: ATGGCGAACTAYAGCCATGC Sreb2-R1094: CTGGATTTTCTGCAGTASAGGAG	Li et al.[54]	Initial denaturation at 95 °C for 4 min, 40 cycles at 95 °C for 30 s (denaturation), 62 °C for 1 min (hybridization) and 72 °C for 90 s (extension), plus a final extension at 72 °C for 5 min
GLYT	Glyt-F559: GGACTGTCMAAGATGACCACMT Glyt-R1562: CCCAAGAGGTTCTTGTTRAAGAT	Li et al.[54]	Initial denaturation at 94 °C for 3 min, 35 cycles at 94 °C for 40 s (denaturation), 56 °C for 40 s (hybridization) and 72 °C for 1 min (extension), plus a final extension at 72 °C for 5 min
PLAG2	Plagl2-F9: CCACACACTCYCCACAGAA Plagl2-R930: TTCTCAAGCAGGTATGAGGTAGA	Li et al.[54]	Initial denaturation at 94 °C for 3 min, 35 cycles at 94 °C for 40 s (denaturation), 64 °C for 40 s (hybridization) and 72 °C for 1 min (extension), plus a final extension at 72 °C for 5 min
MYH6	Myh6-F459: CATMTTYTCCATCTCAGATAATGC Myh6-R1322: CTCACCACCATCCAGTTGAACAT	Li et al.[54]	Initial denaturation at 94 °C for 3 min, 35 cycles at 94 °C for 40 s (denaturation), 58.8 °C for 40 s (hybridization) and 72 °C for 1 min (extension), plus a final extension at 72 °C for 5 min
ZICI	ZicI-F9: GGACGCAGGACCGCARTAYC ZicI-R967: CTGTGTGTGTCCTTTTGTGRATYTT	Li et al.[54]	Initial denaturation at 95 °C for 4 min, 40 cycles at 95 °C for 30 s (denaturation), 62 °C for 1 min (hybridization) and 72 °C for 90 s (extension), plus a final extension at 72 °C for 5 min
TBRI	TbrI-F1: TGTCTACACAGGCTGCGACAT TbrI-R820: GATGTCCTTRGWGCAGTTTTT	Li et al.[54]	Initial denaturation at 95 °C for 4 min, 40 cycles at 95 °C for 30 s (denaturation), 62 °C for 1 min (hybridization) and 72 °C for 90 s (extension), plus a final extension at 72 °C for 5 min

Table 2. Primers and amplification conditions used in analyses of genomic regions in stelliferinae.

Data availability

The data that support the findings of this study will be openly available in GenBank at https://www.ncbi.nlm.nih.gov/genbank/, under the accession numbers provided in Table 1.

Received: 22 August 2024; Accepted: 24 June 2025
Published online: 16 July 2025

References

1. Fricke, R., Eschmeyer, W. N. & van der Laan, R. Eschmeyer's catalog of fishes: genera, species, references (2024). http://researcharchive.calacademy.org/research/ichthyology/catalog/fishcatmain.asp.
2. Nelson, J. S., Grande, T. C. & Wilson, M. V. H. *Fishes of the World* , 5th edn (Wiley, 2016).
3. Parenti, P. An annotated checklist of fishes of the family Sciaenidae. *J. Anim. Divers.* **2**, 1–92 (2020).
4. Santos, S., Gomes, M. F., Ferreira, A. R. S., Sampaio, I. & Schneider, H. Molecular phylogeny of the Western South Atlantic Sciaenidae based on mitochondrial and nuclear data. *Mol. Phylogenet Evol.* **66**, 423–428 (2013).
5. Xu, T., Tang, D., Cheng, Y. & Wang, R. Mitogenomic perspectives into Sciaenid fishes' phylogeny and evolution origin in the new world. *Gene* **539**, 91–98 (2014).
6. Lo, P-C. et al. A multi-gene dataset reveals a tropical new world origin and early miocene diversification of croakers (Perciformes: Sciaenidae). *Mol. Phylogenet Evol.* **88**, 132–143 (2015).
7. Han, X., Jin, S., Han, Z. & Gao, T. The phylogenetic relationships of the family Sciaenidae based on genome-wide data analysis. *Animals* **12**, 3386. https://doi.org/10.3390/ani12233386 (2022).
8. Barbosa, A. J. B., Sampaio, I., Schneider, H. & Santos, S. Molecular phylogeny of weakfish species of the Stellifer group, sciaenidae, Perciformes of the Western South Atlantic based on mitochondrial and nuclear data. *PLOS One*. **9**, e102250. https://doi.org/10.1371/journal.pone.0102250 (2014).
9. Silva, T. F. et al. Phylogeny of the subfamily stelliferinae suggests speciation in *Ophioscion* gill, 1863 (Sciaenidae: Perciformes) in the Western South Atlantic. *Mol. Phylogenet Evol.* **125**, 51–61 (2018).
10. Chao, N. L. A basis for classifying western Atlantic Sciaenidae, Teleostei, Perciformes. *NOAA. Technical Report Circular* **415**, 1–64 (1978).
11. Sasaki, K. Phylogeny of the family Sciaenidae with notes on its zoogeography, teleostei, Perciformes. *Mem. Fac. Fish. Hokkaido Univ.* **36**, 1–137 (1989).
12. Chao, N. L., Carvalho-Filho, A. & Santos, J. A. Five new species of Western Atlantic stardrums, *Stellifer* (Perciformes: Sciaenidae) with a key to Atlantic *Stellifer* species. *Zootaxa* **4991**, 434–466 (2021).

13. Duarte, L. A. G. et al. DNA barcoding and Atlantic reef fishes: the molecular identification of a reef fish community from the Todos Os Santos bay, bahia, Brazil. *Forensic Sci. Int. Genet.* **6**, E284–E285. https://doi.org/10.1016/j.fsigss.2017.09.140 (2017).
14. Da Silva, T. F. et al. Species delimitation by DNA barcoding reveals undescribed diversity in stelliferinae (Sciaenidae). *PLOS One.* **18**, e0296335. https://doi.org/10.1371/journal.pone.0296335 (2023).
15. Araújo, G. S. et al. The Amazon-Orinoco barrier as a driver of reef-fish speciation in the Western Atlantic through time. *J. Biogeogr.* **49**, 1407–1419 (2022).
16. Lessios, H. A. The great American schism: divergence of marine organisms after the rise of the central American isthmus. *Annu. Rev. Ecol. Evol. Syst.* **39**, 63–91 (2008).
17. Steph, S. et al. Changes in Caribbean surface hydrography during the pliocene shoaling of the central American seaway. *Paleoceanography* **21**, PA4221. https://doi.org/10.1029/2004PA001092 (2006).
18. O'Dea, A. et al. Formation of the isthmus of Panama. *Sci. Adv.* **2**, e1600883. https://doi.org/10.1126/sciadv.1600883 (2016).
19. Figueiredo, J., Hoorn, C., van der Ven, P. & Soares, E. Late miocene onset of the Amazon river and the Amazon deep-sea fan: evidence from the Foz do Amazonas basin. *Geology* **37**, 619–622 (2009).
20. Milliman, J. D. & Meade, R. H. World-wide delivery of river sediment to the oceans. *J. Geol.* **91**, 1–21 (1983).
21. Robertson, D. R., Karg, F., de Moura, R. L., Victor, B. C. & Bernardi, G. Mechanisms of speciation and faunal enrichment in Atlantic parrotfishes. *Mol. Phylogenet Evol.* **40**, 795–807 (2006).
22. Pinheiro, H. T. et al. South-western Atlantic reef fishes: zoogeographical patterns and ecological drivers reveal a secondary biodiversity centre in the Atlantic ocean. *Divers. Distrib.* **24**, 951–965 (2018).
23. Arcila, D. et al. Testing the utility of alternative metrics of branch support to address the ancient evolutionary radiation of tunas, stromateoids, and allies (Teleostei: Pelagiaria). *Syst. Biol.* **70**, 1123–1144 (2021).
24. Tea, Y-K. et al. Phylogenomic analysis of concatenated ultraconserved elements reveals the recent evolutionary radiation of the Fairy wrasses (Teleostei: labridae: *Cirrhilabrus*). *Syst. Biol.* **71**, 1–12 (2022).
25. Grove, J. S. & Lavenberg, R. J. *The Fishes of the Galápagos Islands* (Stanford University Press, 1997).
26. Chao, N. L. Corvinas barbiches, bombaches, corvinatas, corvinetas, corvinillas, lambes, pescadillas, roncachos, verrugatos in *Guía FAO para la identificación de especies para los fines de la pesca. Pacífico centro-oriental. Volumen III. Vertebrados - Parte 2* (eds Fischer, W., Krupp, F., Schneider, W., Sommer, C., Carpenter, K. E. & Niem, V. H.) 1427–1518 (FAO, Rome, 1995).
27. Froese, R. & Pauly, D. (eds). *FishBase*. June (2025). https://www.fishbase.org (accessed 16 June 2025).
28. Andrade-Santos, J., Rosa, R. S. & Ramos, T. P. A. Spotting mistakes: reappraisal of spotted drum *Stellifer punctatissimus* (Meek & Hildebrand, (Teleostei: Sciaenidae) reveals species misidentification trends and suggests latitudinal sexual dimorphism. *Zool.* **165**, 126180 (1925). https://doi.org/10.1016/j.zool.2024.126180 (2024).
29. Ossa-Hernández, N., Ballen, G. A., Tavera, J. & P, A. A. & Phylogenetic and biogeographic history of the snooks (Centropomidae: Carangiformes) spanning the closure of the isthmus of Panama. *J. Biogeogr.* **0**, 1–13. https://doi.org/10.1111/jbi.15018 (2024).
30. Duque-Caro, H. Neogene stratigraphy, paleoceanography and paleobiogeography in Northwest South America and the evolution of the Panama seaway. *Palaeogeogr Palaeoclimatol Palaeoecol.* **77**, 203–234 (1990).
31. Keigwin, L. Isotopic paleoceanography of the Caribbean and East pacific: role of Panama uplift in late neogene time. *Science* **217**, 350–353 (1982).
32. Groeneveld, J. et al. Foraminiferal mg/ca increase in the Caribbean during the pliocene: Western Atlantic warm pool formation, salinity influence, or diagenetic overprint? *Geochem. Geophys. Geosyst.* **9** (23). https://doi.org/10.1029/2006GC001564 (2008).
33. Swart, B. L., Heyden, V. D., Bester-van der Merwe, S., Roodt-Wilding, R. & A. & Molecular systematics and biogeography of the circumglobally distributed genus *Seriola* (Pisces: Carangidae). *Mol. Phylogenet Evol.* **93**, 274–280 (2015).
34. Thacker, C. E. Patterns of divergence in fish species separated by the isthmus of Panama. *BMC Evol. Biol.* **17.** https://doi.org/10.1186/s12862-017-0957-4 (2017).
35. Tavera, J. J. & Wainwright, P. C. Geography of speciation affects rate of trait divergence in haemulid fishes. *Proc. R Soc. Lond. B Biol. Sci.* **286**, 20182852. https://doi.org/10.1098/rspb.2018.2852 (2019).
36. Aroca, A. K., Tavera, J. & Torres, Y. Molecular and morphological evaluation of the bonnethead shark complex *Sphyrna tiburo* (Carcharhiniformes: Sphyrnidae). *Environ. Biol. Fishes.* **105**, 1643–1658 (2022).
37. Lieske, E. & Myers, R. *Collins Pocket Guide - Coral Reef Fishes of the Indo-Pacific & Caribbean* (Haper Collins, 1994).
38. Curtin, T. B. & Legeckis, R. V. Physical observations in the plume region of the Amazon river during peak discharge - I. Surface variability. *Cont. Shelf Res.* **6**, 31–51 (1986).
39. Nittrouer, C. A. & DeMaster, D. J. Sedimentary processes on the Amazon continental shelf: past, present and future research. *Cont. Shelf Res.* **6**, 5–30 (1986).
40. Masson, S. & Delecluse, P. Influence of the Amazon river runoff of the tropical Atlantic. *Phys. Chem. Earth Part. B Hydrology Oceans Atmos.* **26**, 137–142 (2001).
41. Rocha, L. A., Bass, A. L., Robertson, D. R. & Bowen, B. W. Adult habitat preferences, larval dispersal, and the comparative phylogeography of three Atlantic surgeon fishes (Teleostei: Acanthuridae). *Mol. Ecol.* **11**, 243–251 (2002).
42. Dias, R. M. et al. Different speciation processes in a cryptobenthic reef fish from the Western tropical Atlantic. *Hydrobiologia* **837**, 133–147 (2019).
43. Volk, D. R., Konvalina, J. D., Floeter, S. R., Ferreira, C. E. L. & Hoffman, E. A. Going against the flow: barriers to gene flow impact patterns of connectivity in cryptic coral reef gobies throughout the Western Atlantic. *J. Biogeogr.* **48**, 427–439 (2021).
44. Menezes, N. A. & Figueiredo, J. L. *Manual De Peixes Marinhos Do Sudeste Do Brasil. Vol. IV. Teleostei (3)* (Museu de Zoologia da Universidade de São Paulo, São Paulo, 1980).
45. Cervigón, F. et al. *FAO Species Identification Sheets for Fishery Purposes. Field Guide To the Commercial Marine and Brackish-Water Resources of the Northern Coast of South America* (FAO, Rome, 1993).
46. Bussing, W. A. & López, M. I. *Peces Desmersales Y Pelágicos Costeros Del Pacífico De Centroamérica Meridional* (Editorial de la Universidad de Costa Rica, 2011).
47. Ward, R. D., Zemlak, T. S., Innes, B. H., Last, P. R. & Hebert, P. D. N. DNA barcoding australia's fish species. *Phil Trans. R Soc. B.* **360**, 1847–1857 (2005).
48. Sevilla, R. G. et al. Primers and polymerase chain reaction conditions for DNA barcoding teleost fish based on the mitochondrial cytochrome b and nuclear rhodopsin genes. *Mol. Ecol. Notes.* **7**, 730–734 (2007).
49. Palumbi, S. R. Nucleic acids II: the polymerase chain reaction in Molecular Systematics (eds Hillis, D. & Moritz, C.) 2rd edn. 205–247 (Sinauer, 1996).
50. Chen, W-J., Miya, M., Saitoh, K. & Mayden, R. L. Phylogenetic utility of two existing and four novel nuclear gene loci in reconstructing tree of life of ray-finned fishes: the order Cypriniformes (Ostariophysi) as a case study. *Gene* **423**, 125–134 (2008).
51. Chen, W-J., Lavoué, S. & Mayden, R. L. Evolutionary origin and early biogeography of otophysan fishes (Ostariophysi: Teleostei). *Evolution* **67**, 2218–2239 (2013).
52. Li, C. & Ortí, G. Molecular phylogeny of Clupeiformes (Actinopterygii) inferred from nuclear and mitochondrial DNA sequences. *Mol. Phylogenet Evol.* **44**, 386–398 (2007).
53. López, J. A., Chen, W-J. & Ortí, G. Esociform phylogeny. *Copeia* **2004**, 449–464 (2004).
54. Li, C., Ortí, G., Zhang, G. & Lu, G. A practical approach to phylogenomics: the phylogeny of ray-finned fish (Actinopterygii) as a case study. *BMC Evol. Biol.* **7.** https://doi.org/10.1186/1471-2148-7-44 (2007).
55. Paithankar, K. R. & Prasad, K. S. N. Precipitation of DNA by polyethylene glycol and ethanol. *Nucleic Acids Res.* **19**, 1346 (1991).

56. Sanger, F., Nicklen, S. & Coulson, A. R. DNA sequencing with chain-terminating inhibitors. *Proc. Natl. Acad. Sci. U.S.A.* **74**, 5463–5467 (1977).
57. Hall, A. T BioEdit: a user friendly biological sequence alignment editor and analysis program for windows 95/98/NT. *Nucl. Acids Symp. Ser.* **41**, 95–98 (1999).
58. Thompson, J. D., Higgins, D. G. & Gibson, T. J. CLUSTAL W: improving the sensitivity of progressive multiple sequence alignment through sequence weighting, position-specific gap penalties and weight matrix choice. *Nucleic Acids Res.* **22**, 4673–4680 (1994).
59. Vaidya, G., Lohman, D. J. & Meier, R. SequenceMatrix: concatenation software for the fast assembly of multi-gene datasets with character set and codon information. *Cladistics* **27**, 171–180 (2011).
60. Lanfear, R., Frandsen, P. B., Wright, A. M., Senfeld, T. & Calcott, B. PartitionFinder 2: new methods for selecting partitioned models of evolution for molecular and morphological phylogenetic analyses. *Mol. Biol. Evol.* **34**, 772–773 (2017).
61. Nguyen, L. T., Schmidt, H. A., von Haeseler, A. & Bui, Q. M. IQ-TREE: a fast and effective stochastic algorithm for estimating maximum likelihood phylogenies. *Mol. Biol. Evol.* **32**, 268–274 (2015).
62. Kalyaanamoorthy, S., Minh, B., Wong, T., von Haeseler, A. & Jermiin, L. S. ModelFinder: fast model selection for accurate phylogenetic estimates. *Nat. Methods*. **14**, 587–589 (2017).
63. Ronquist, F. & Huelsenbeck, J. P. MrBayes 3: bayesian phylogenetic inference under mixed models. *Bioinformatics* **19**, 1572–1574 (2003).
64. Zhou, J., Liu, X., Stones, D. S., Xie, Q. & Wang, G. MrBayes on a graphics processing unit. *Bioinformatics* **27**, 1255–1261 (2011).
65. Rambaut, A., Drummond, A. J., Xie, D., Baele, G. & Suchard, M. A. Posterior summarization in bayesian phylogenetics using tracer 1.7. *Syst. Biol.* **67**, 901–904 (2018).
66. Douglas, J., Jiménez-Silva, C. L. & Bouckaert, R. StarBeast3: adaptive parallelized bayesian inference under the multispecies coalescent. *Syst. Biol.* **71**, 901–916 (2022).
67. Bouckaert, R. et al. BEAST 2.5: an advanced software platform for bayesian evolutionary analysis. *PLOS Comput. Biol.* **15**, e1006650. https://doi.org/10.1371/journal.pcbi.1006650 (2019).
68. Nolf, D. & Aguilera, O. Fish otoliths from the cantaure formation (Early miocene of Venezuela). *Bull. De L'Institut Royal Des. Sci. Nat. De Belgique Sci. De La. Terre*. **68**, 237–262 (1998).
69. Aguilera, O. A., Schwarzhans, W. & Béarez, P. Otoliths of the Sciaenidae from the neogene of tropical America. *Palaeo Ichthyol.* **14**, 7–90 (2016).
70. Zhang, C., Rabiee, M., Sayyari, E. & Mirarab, S. ASTRAL-III: polynomial time species tree reconstruction from partially resolved gene trees. *BMC Bioinform.* **19**, 153. https://doi.org/10.1186/s12859-018-2129-y (2018).
71. Stöver, B. C. & Müller, K. F. TreeGraph 2: combining and visualizing evidence from different phylogenetic analyses. *BMC Bioinform.* **11**, 7. https://doi.org/10.1186/1471-2105-11-7 (2010).
72. Yang, Z. & Rannala, B. Bayesian species delimitation using multilocus sequence data. *Proc. Natl. Acad. Sci. U S A.* **107**, 9264–9269 (2010).
73. Yang, Z. The BPP program for species tree Estimation and species delimitation. *Curr. Zool.* **61**, 854–865 (2015).
74. Matzke, N. J. BioGeoBEARS: biogeography with bayesian (and likelihood) evolutionary analysis in R Scripts. R Packag. version 0.2. (2013).
75. Matzke, N. J. Probabilistic historical biogeography: new models for founder-event speciation, imperfect detection, and fossils allow improved accuracy and model-testing. *Front. Biogeogr.* **5**, 242–248 (2013).
76. Robertson, D. R. & Cramer, K. L. Shore fishes and biogeographic subdivisions of the tropical Eastern Pacific. *Mar. Ecol. Prog Ser.* **380**, 1–17 (2009).
77. Ree, R. H. & Smith, S. A. Maximum likelihood inference of geographic range evolution by dispersal, location extinction, and cladogenesis. *Syst. Biol.* **57**, 4–14 (2008).
78. Ronquist, F. Dispersal-vicariance analysis: a new approach to the quantification of historical biogeography. *Syst. Biol.* **46**, 195–203 (1997).
79. Landis, M. J., Matzke, N. J., Moore, R. B. & Huelsenbeck, J. P. Bayesian analysis of biogeography when the number of areas is large. *Syst. Biol.* **62**, 789–804 (2013).
80. Matzke, N. J. Model selection in historical biogeography reveals that founder-event speciation is a crucial process in Island clades. *Syst. Biol.* **63**, 951–970 (2014).

Acknowledgements

The authors are grateful to Aurycéia Guimarães-Costa, Gabriele Malcher, and Adam Rick Bessa for their assistance in the analyses from the present study.

Author contributions

The study conception and design were performed by T.F.S. and S.S. The methodology, validation, formal analysis, investigation and data curation were performed by T.F.S., I.S., A.A., O.D., and S.S. The original draft of the manuscript was written by TFS, and all authors commented on previous versions of the manuscript. All authors have read and agreed to the published version of the manuscript.

Competing interests

The authors declare no competing interests.

Additional information

Supplementary Information The online version contains supplementary material available at https://doi.org/10.1038/s41598-025-08793-7.

Correspondence and requests for materials should be addressed to S.S.

Reprints and permissions information is available at www.nature.com/reprints.

Publisher's note Springer Nature remains neutral with regard to jurisdictional claims in published maps and institutional affiliations.

Terms and Conditions

Springer Nature journal content, brought to you courtesy of Springer Nature Customer Service Center GmbH (“Springer Nature”).
Springer Nature supports a reasonable amount of sharing of research papers by authors, subscribers and authorised users (“Users”), for small-scale personal, non-commercial use provided that all copyright, trade and service marks and other proprietary notices are maintained. By accessing, sharing, receiving or otherwise using the Springer Nature journal content you agree to these terms of use (“Terms”). For these purposes, Springer Nature considers academic use (by researchers and students) to be non-commercial.
These Terms are supplementary and will apply in addition to any applicable website terms and conditions, a relevant site licence or a personal subscription. These Terms will prevail over any conflict or ambiguity with regards to the relevant terms, a site licence or a personal subscription (to the extent of the conflict or ambiguity only). For Creative Commons-licensed articles, the terms of the Creative Commons license used will apply.
We collect and use personal data to provide access to the Springer Nature journal content. We may also use these personal data internally within ResearchGate and Springer Nature and as agreed share it, in an anonymised way, for purposes of tracking, analysis and reporting. We will not otherwise disclose your personal data outside the ResearchGate or the Springer Nature group of companies unless we have your permission as detailed in the Privacy Policy.
While Users may use the Springer Nature journal content for small scale, personal non-commercial use, it is important to note that Users may not:

1. use such content for the purpose of providing other users with access on a regular or large scale basis or as a means to circumvent access control;
2. use such content where to do so would be considered a criminal or statutory offence in any jurisdiction, or gives rise to civil liability, or is otherwise unlawful;
3. falsely or misleadingly imply or suggest endorsement, approval , sponsorship, or association unless explicitly agreed to by Springer Nature in writing;
4. use bots or other automated methods to access the content or redirect messages
5. override any security feature or exclusionary protocol; or
6. share the content in order to create substitute for Springer Nature products or services or a systematic database of Springer Nature journal content.

In line with the restriction against commercial use, Springer Nature does not permit the creation of a product or service that creates revenue, royalties, rent or income from our content or its inclusion as part of a paid for service or for other commercial gain. Springer Nature journal content cannot be used for inter-library loans and librarians may not upload Springer Nature journal content on a large scale into their, or any other, institutional repository.
These terms of use are reviewed regularly and may be amended at any time. Springer Nature is not obligated to publish any information or content on this website and may remove it or features or functionality at our sole discretion, at any time with or without notice. Springer Nature may revoke this licence to you at any time and remove access to any copies of the Springer Nature journal content which have been saved.
To the fullest extent permitted by law, Springer Nature makes no warranties, representations or guarantees to Users, either express or implied with respect to the Springer nature journal content and all parties disclaim and waive any implied warranties or warranties imposed by law, including merchantability or fitness for any particular purpose.
Please note that these rights do not automatically extend to content, data or other material published by Springer Nature that may be licensed from third parties.
If you would like to use or distribute our Springer Nature journal content to a wider audience or on a regular basis or in any other manner not expressly permitted by these Terms, please contact Springer Nature at

onlineservice@springernature.com